Elaborating H-bonding effect and excited state intramolecular proton transfer of 2-(2-hydroxyphenyl) benzothiazole based D-π-A fluorescent dye

Xiu-Min Liu [1a], Yin Yu [1a], Shu-Ying Xu[2], Xue-Hai Ju [1*]

[1] Key Laboratory of Soft Chemistry and Functional Materials of MOE, School of Chemistry and Chemical Engineering, Nanjing University of Science and Technology, Nanjing 210094, P. R. China

2 Institute of Research and Development Design, Xinxiang Aviation Industry (Group) CO., LTD, Xinxiang 453000, P. R. China

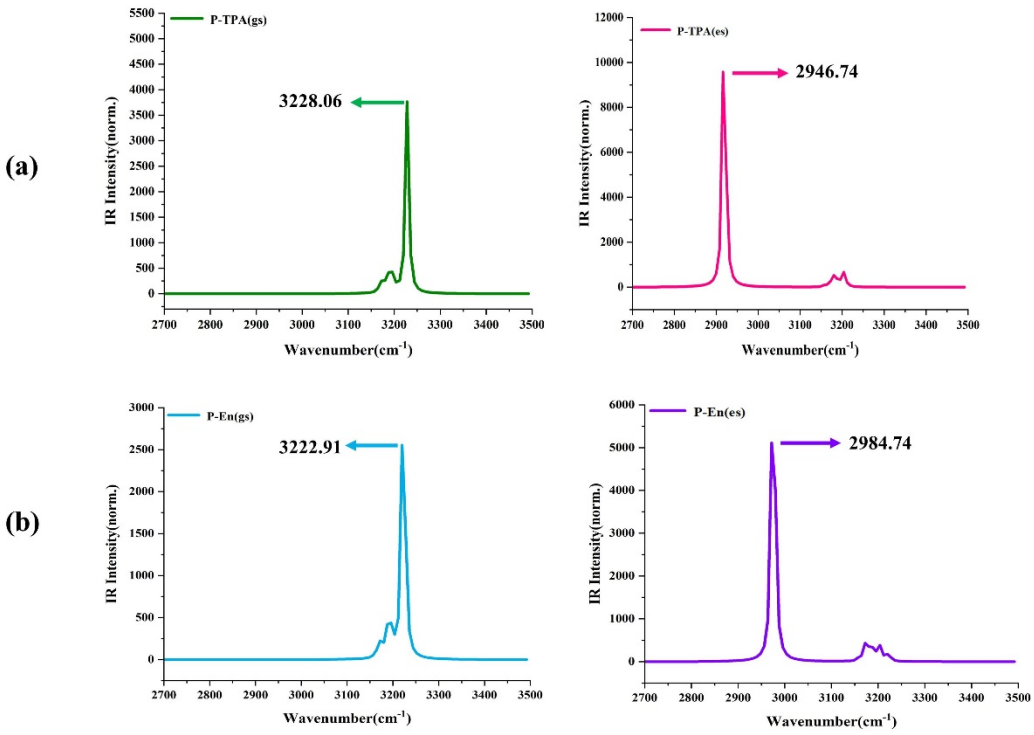

Fig. S1 Calculated stretching vibrational frequencies of the bond O_1-H_2 in the S_0 and S_1 state. (a) P-TPA molecules; (b) P-En molecules

* Corresponding author. xhju@njust.edu.cn (Xue-Hai Ju)
a These authors contributed equally

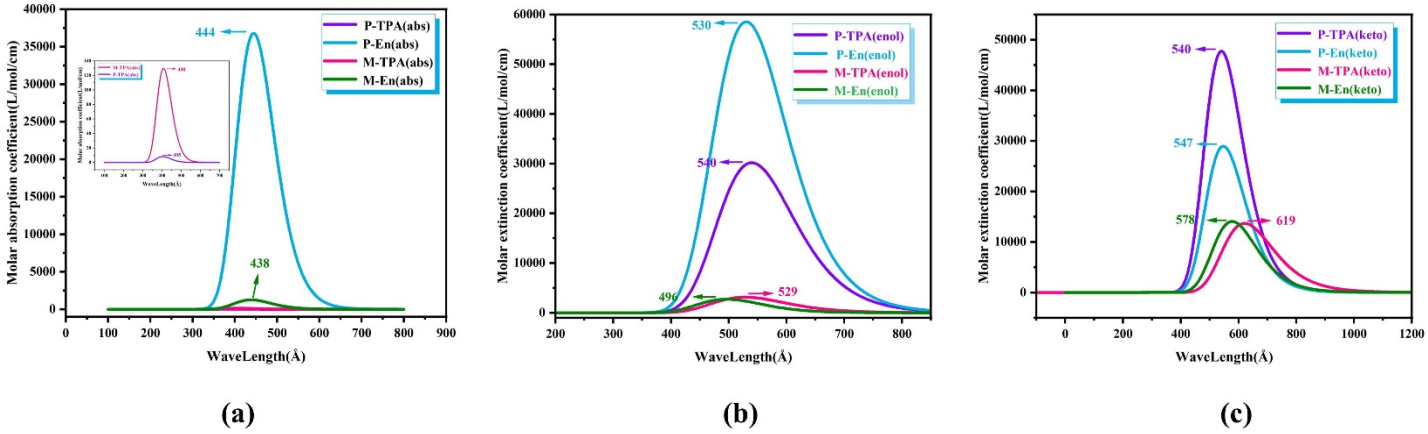

Fig. S2 Calculated absorption and fluorescence spectra for P-TPA, P-En, M-TPA and M-En molecules. (a) Absorption spectra; (b) Emission spectra of enol forms; (c)Emission spectra of keto forms

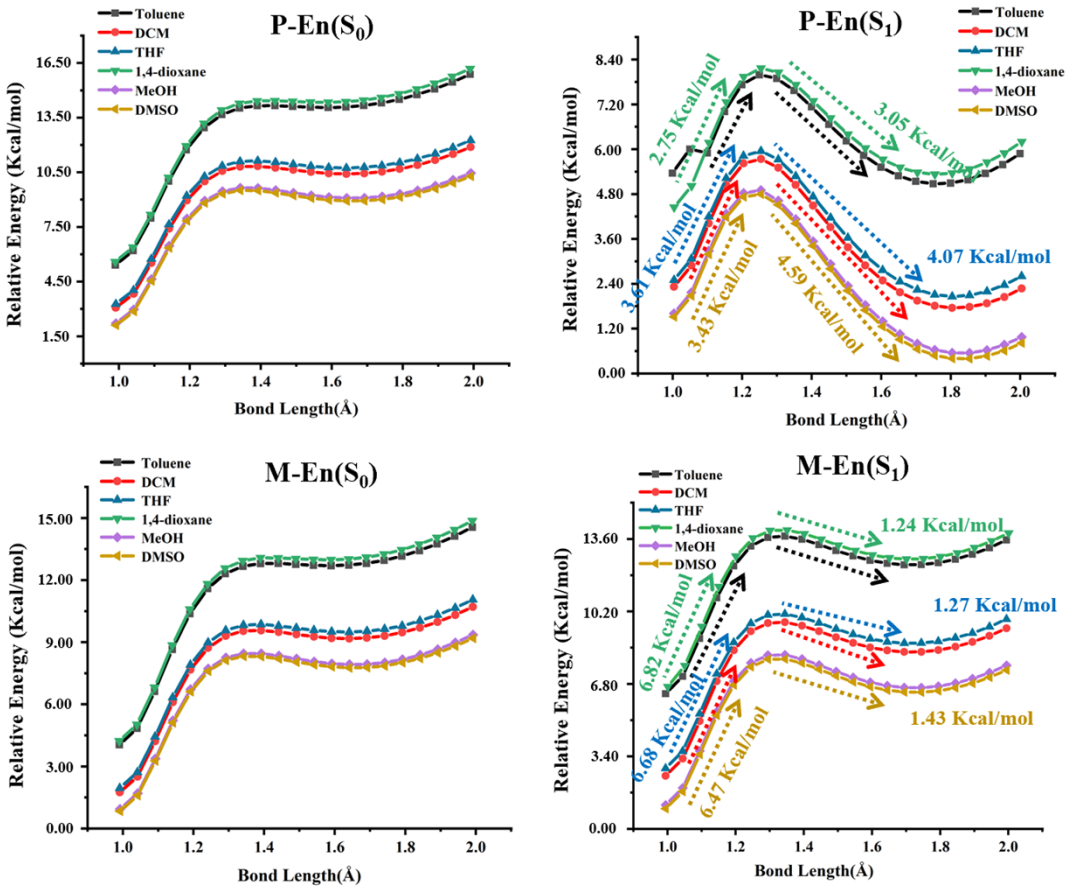

Fig. S3 Potential energy curves of S_0 and S_1 states of P-En and M-En as a function O_1–

H_2 bond length in different kinds of solvents (Toluene, DCM, THF, 1,4-dioxane, MeOH, DMSO)

Table S1 lists the hydrogen-bond lengths of four derivates in the S_0 and S_1 states. Herein, the key atoms involved in forming hydrogen bonds are numbered 1-3. The O_1–H_2 bond lengths of P-TPA and M-TPA are 0.9919 Å and 0.9921 Å in the S_0 state, increasing to 1.0071 Å and 0.9951 Å in the S_1 state, respectively. The $H_2\cdots N_3$ distances of P-TPA and M-TPA are 1.7339 Å and 1.7314 Å in the S_0 state, decreasing to 1.6626 Å and 1.7141 Å in the S_1 state, respectively. Moreover, upon photo-excitation process the hydrogen-bond angles $\delta(O_1–H_2–N_3)$ of P-TPA and M-TPA increases from 146.99° and 147.26° to 150.99° and 149.55°, respectively. Similar results were found for P-En and M-En, and see supplementary information for detailed analysis.

Similarly, for molecules, the O_1–H_2 bond lengths increase from 0.9918 Å and 0.9919 Å in the S_0 state to 1.0039 Å and 0.9947 Å in the S_1 state, respectively; the distances of $H_2\cdots N_3$ shorten from 1.7326 Å and 1.7320 Å in the S_0 state to 1.6741 Å and 1.7164 Å in the S_1 state, respectively. The hydrogen bond angles $\delta(O_1–H_2–N_3)$ of P-En and M-En separately increase from 147.04° to 147.13° in the S_0 state to 150.89° and 148.72° in the S_1 state. The alterations in the bond parameters demonstrate that the intramolecular HB strengths of four molecules are strengthened during the photo-excitation process. Moreover, compared with the meta-substitution, the hydrogen bond enhancement effect of para-substitution is more obvious. Thus, the presence of different substitution positions and excited states will affect ESIPT

As shown in Fig. 6, the O_1–H_2 bond lengths and distances of $H_2\cdots N_3$ separately increase and shorten during the photo-excitation process, which confirms the ESIHB strengthening mechanism. Additionally, when we investigate the effect of different triphenylamine and anthracenyl groups position on hydrogen bond interaction, notice from Fig. 6 that the O_1–H_2 bond lengths of P-TPA and P-En are shorter than that of M-TPA and M-En in the S_0 state, respectively; the $H_2\cdots N_3$ distances of P-TPA and P-En

are longer than that of M-TPA and M-En in S_0 state, respectively. It indicates that the intramolecular hydrogen bonds are stronger in S_0 state as triphenylamine and anthracenyl groups locate at meta-position. On the contrary, the excited-state intramolecular hydrogen bonds of para-substitution are stronger by comparing hydrogen-bond parameters. Upon photoexcitation process, the O_1–H_2 bond lengths of P-TPA and P-En molecules increase by 0.0152 Å and 0.0121 Å, respectively; the O_1–H_2 bond lengths of M-TPA and M-En molecules increase by 0.0030 Å and 0.0028 Å respectively in Fig. 6. Meanwhile, the $H_2\cdots N_3$ distances of P-TPA and P-En molecules reduce by 0.0713 Å and 0.0585 Å, respectively; the $H_2\cdots N_3$ distances of M-TPA and M-En molecules reduce by 0.0173 Å and 0.0156 Å respectively in Fig. 6. We find that the changes of intramolecular hydrogen-bond parameters are more drastic as triphenylamine group locates at para-position. Compared with the meta-substitution, the para-substitution of triphenylamine group has the greater impact on intramolecular hydrogen bond.

Table S1 Bond lengths (Å) and angles (°) of S_0 and S_1 states for the studied molecules P-TPA, M-TPA, P-En and M-En in dimethyl sulfoxide solvent

Species	O_1-H_2		$H_2\cdots N_3$		$\delta(O_1$-H_2-$N_3)$	
States	S_0	S_1	S_0	S_1	S_0	S_1
P-TPA	0.9919	1.0071	1.7339	1.6626	146.99	150.99
M-TPA	0.9921	0.9951	1.7314	1.7141	147.26	149.55
P-En	0.9918	1.0039	1.7326	1.6741	147.04	150.89
M-En	0.9919	0.9947	1.7320	1.7164	147.13	148.72

Table S2 Observed absorption and emission spectra of P-TPA in different solvent, as well as Stocks' shifts and the oscillator strengths of N* and K*

Solvent	λ_{abs} (nm)	λ_{em} (nm)	Stokes' shifts (nm)	Oscillator Strengths	
				N*	K*
Toluene	442	506	64	0.879	0.598
Dichloromethane (DCM)	444	521	77	1.318	1.024

Tetrahydrofuran (THF)	443	519	76	1.285	0.987
1,4-dioxane	441	505	64	0.836	0.565
Methanol (MeOH)	443	529	86	1.433	1.162
Dimethyl sulfoxide (DMSO)	405	540	135	1.445	1.179

Table S3 Observed absorption and emission spectra of M-TPA in different solvent, as well as Stocks' shifts and the oscillator strengths of N* and K*

Solvent	λ_{abs} (nm)	λ_{em} (nm)	Stokes' shifts (nm)	Oscillator Strengths	
				N*	K*
Toluene	439	518	79	0.058	0.287
Dichloromethane (DCM)	438	525	87	0.072	0.326
Tetrahydrofuran (THF)	438	525	87	0.071	0.323
1,4-dioxane	439	518	79	0.058	0.283
Methanol (MeOH)	438	528	90	0.077	0.336
Dimethyl sulfoxide (DMSO)	408	529	121	0.077	0.337

Table S4 Observed absorption and emission spectra of P-En in different solvent, as well as Stocks' shifts and the oscillator strengths of N* and K*

Solvent	λ_{abs} (nm)	λ_{em} (nm)	Stokes' shifts (nm)	Oscillator Strengths	
				N*	K*
Toluene	411	513	102	0.547	0.224
Dichloromethane (DCM)	407	532	125	0.693	0.693
Tetrahydrofuran (THF)	407	530	123	0.682	0.573
1,4-dioxane	412	480	68	0.551	0.008
Methanol (MeOH)	405	538	133	0.740	0.703
Dimethyl sulfoxide (DMSO)	444	530	86	0.745	0.714

Table S5 Observed absorption and emission spectra of M-En in different solvent, as well as Stocks' shifts and the oscillator strengths of N* and K*

Solvent	λ_{abs} (nm)	λ_{em} (nm)	Stokes' shifts (nm)	Oscillator Strengths	
				N*	K*
Toluene	412	484	72	0.002	0.200
Dichloromethane (DCM)	409	497	88	0.057	0.301
Tetrahydrofuran (THF)	409	497	88	0.055	0.291
1,4-dioxane	412	499	87	0.037	0.037
Methanol (MeOH)	408	496	88	0.066	0.342
Dimethyl sulfoxide (DMSO)	438	496	58	0.067	0.347

Table S6 Gibbs free energy values (Hartree) of normal, TS and isomer structures of P-TPA molecules in six solvents, as well as the proton-transfer activation energy barriers (Kcal/mol) in the S_0 and S_1 states

States	Solvent	Normal (Hartree)	TS (Hartree)	Barrier (Kcal/mol)	Isomer (Hartree)	Reversed barrier (Kcal/mol)
GS	Toluene	–1777.876653	–1777.861925	9.24	–1777.862061	0.08
	DCM	–1777.881047	–1777.867923	8.23	–1777.868621	0.43
	THF	–1777.880652	–1777.867385	8.33	–1777.868031	0.41
	1,4-dioxane	–1777.876301	–1777.861434	9.32	–1777.861587	0.09
	MeOH	–1777.882596	–1777.870024	7.89	–1777.870940	0.58
	DMSO	–1777.882789	–1777.870279	7.85	–1777.871228	0.60
ES	Toluene	–1777.779663	–1777.774045	3.52	–1777.778535	2.81
	DCM	–1777.784741	–1777.779654	3.19	–1777.786013	3.99
	THF	–1777.784285	–1777.779151	3.22	–1777.785343	3.88
	1,4-dioxane	–1777.779257	–1777.773596	3.55	–1777.777931	2.72
	MeOH	–1777.786525	–1777.781625	3.07	–1777.788621	4.39
	DMSO	–1777.786746	–1777.781869	3.06	–1777.788942	4.43

Table S7 Gibbs free energy values (Hartree) of normal, TS and isomer structures of M-TPA molecules in six solvents, as well as the proton-transfer activation energy barriers (Kcal/mol) in the S_0 and S_1 states

States	Solvent	Normal (Hartree)	TS (Hartree)	Barrier (Kcal/mol)	Isomer (Hartree)	Reversed barrier (Kcal/mol)
GS	Toluene	–1777.875183	–1777.860663	9.11	–1777.860895	0.15

	DCM	–1777.879547	–1777.866613	8.11	–1777.867370	0.47
	THF	–1777.879155	–1777.866078	8.21	–1777.866784	0.44
	1,4-dioxane	–1777.874833	–1777.860181	9.19	–1777.860340	0.10
	MeOH	–1777.881087	–1777.868685	7.78	–1777.869673	0.62
	DMSO	–1777.881278	–1777.868938	7.74	–1777.869943	0.63
ES	Toluene	–1777.780400	–1777.769146	7.06	–1777.770570	0.89
	DCM	–1777.787256	–1777.776652	6.65	–1777.778608	1.23
	THF	–1777.786621	–1777.775947	6.70	–1777.777847	1.19
	1,4-dioxane	–1777.779876	–1777.768576	7.09	–1777.769965	0.87
	MeOH	–1777.789757	–1777.779447	6.47	–1777.781643	1.37
	DMSO	–1777.790068	–1777.779797	6.44	–1777.782027	1.39

Table S8 Gibbs free energy values (Hartree) of normal, TS and isomer structures of P-En molecules in six solvents, as well as the proton-transfer activation energy barriers (Kcal/mol) in the S_0 and S_1 states

States	Solvent	Normal (Hartree)	TS (Hartree)	Barrier (Kcal/mol)	Isomer (Hartree)	Reversed barrier (Kcal/mol)
GS	Toluene	–1567.643497	–1567.62890	9.15	–1567.629079	0.11
	DCM	–1567.647407	–1567.634452	8.12	–1567.635154	0.44
	THF	–1567.647052	–1567.633949	8.22	–1567.634597	0.40
	1,4-dioxane	–1567.643187	–1567.628449	9.24	–1567.628601	0.09
	MeOH	–1567.648807	–1567.636415	7.77	–1567.637350	0.52
	DMSO	–1567.648982	–1567.636655	7.73	–1567.637624	0.60
ES	Toluene	–1567.541065	–1567.536683	2.75	–1567.541541	3.04
	DCM	–1567.546133	–1567.540434	3.57	–1567.547076	4.16
	THF	–1567.545831	–1567.540084	3.60	–1567.546568	4.06
	1,4-dioxane	–1567.542592	–1567.536389	3.89	–1567.541120	2.96
	MeOH	–1567.547323	–1567.541828	3.44	–1567.549083	4.55
	DMSO	–1567.54747	–1567.542004	3.43	–1567.549333	4.59

Table S9 Gibbs free energy values (Hartree) of normal, TS and isomer structures of M-En molecules in six solvents, as well as the proton-transfer activation energy barriers (Kcal/mol) in the S_0 and S_1 states

States	Solvent	Normal (Hartree)	TS (Hartree)	Barrier (Kcal/mol)	Isomer (Hartree)	Reversed barrier (Kcal/mol)

GS	Toluene	–1567.643257	–1567.628658	9.16	–1567.628836	0.11
	DCM	–1567.647090	–1567.634048	8.18	–1567.634714	0.41
	THF	–1567.646746	–1567.633562	8.27	–1567.634182	0.38
	1,4-dioxane	–1567.642950	–1567.628211	9.24	–1567.628367	0.09
	MeOH	–1567.648436	–1567.635915	7.85	–1567.636791	0.54
	DMSO	–1567.648602	–1567.636141	7.81	–1567.637037	0.56
ES	Toluene	–1567.545675	–1567.534804	6.82	–1567.536785	1.24
	DCM	–1567.551341	–1567.540744	6.64	–1567.54280	1.29
	THF	–1567.550829	–1567.540178	6.68	–1567.542194	1.26
	1,4-dioxane	–1567.54520	–1567.534393	6.78	–1567.536395	1.25
	MeOH	–1567.553354	–1567.543003	6.49	–1567.545263	1.41
	DMSO	–1567.553605	–1567.543288	6.47	–1567.545577	1.43

The electron donor substituents can provide electrons to the reaction center through conjugation, which makes it easier for electron transfer reaction to occur, thus speeding up the reaction rate. The electron-withdrawing groups generally reduce the electron cloud density of the entire system. In this section, the substitution effects of benzothiazole on electron donor groups and electron withdrawing groups (para-and meta-triphenylamine and DNP) are systematically investigated to regulate the photophysical properties and hydrogen bonding behavior of molecules in DMSO solvents, as shown in Figure S4. They are denoted by P-TPA, M-TPA, P-DNP, M-DNP (Figure S5). Among them, the nitrogen atom in the center of triphenylamine has a lone electron pair, which can be regarded as the iso-electron body of carbon ion, and DNP group has a strong electron absorption ability.

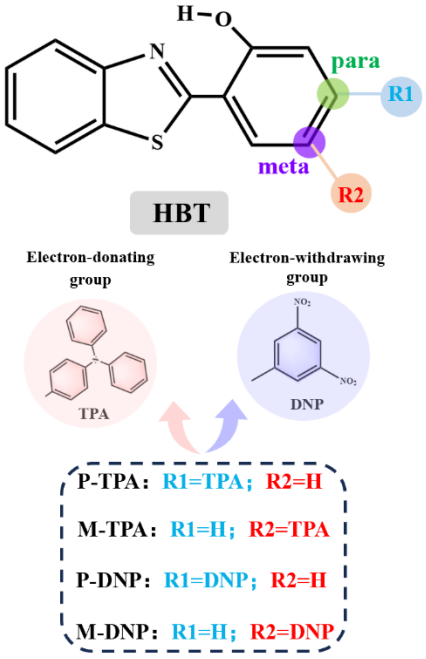

Fig. S4 Chemical structures of P-TPA, M-TPA, P-DNP and M-DNP

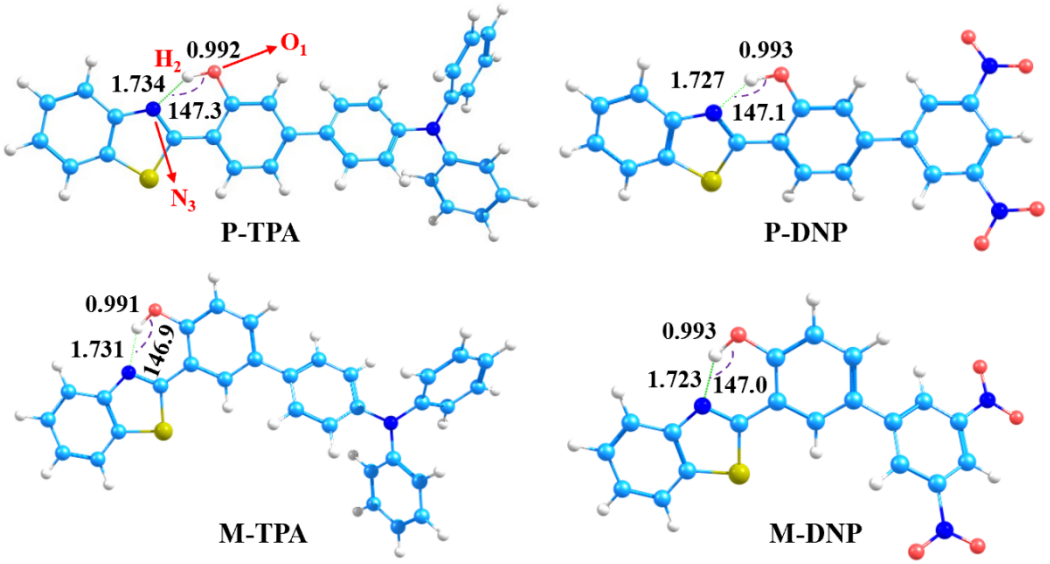

Fig. S5 Geometric configurations and bond parameters of P-TPA, M-TPA, P-DNP and M-DNP. (cyan: C atom; red: O atom; blue: N atom; and white: H atom)

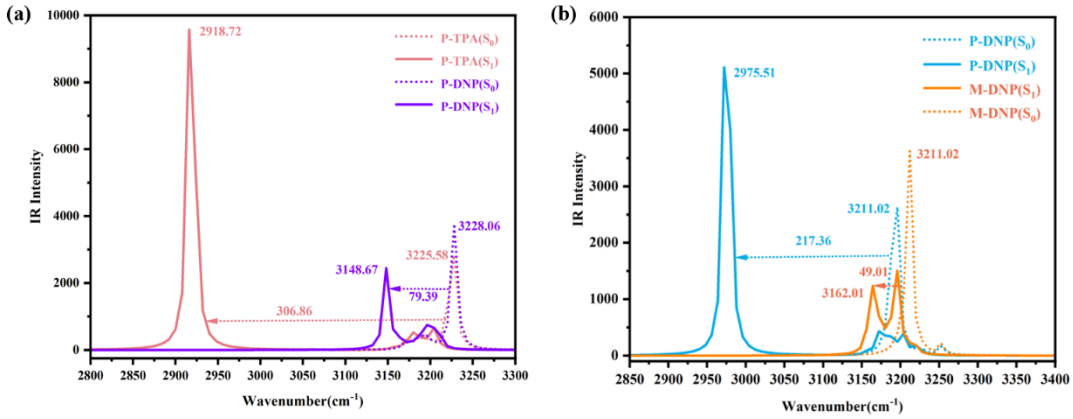

Fig. S6 Simulated IR spectra of the studied molecules (P-TPA, M-TPA, P-DNP and M-DNP)

Indeed, analyzing the strength of hydrogen bonds by comparing the changes in the vibrational frequency of the hydroxyl group in the IR spectra after light excitation is a widely used method. When the strength of a hydrogen bond changes or when a new hydrogen bond forms, it impacts the vibrational energy of the hydroxyl group. This impact is observable as shifts in the IR absorption peaks. The simulated IR spectra of the molecules are presented in Figure S6. As shown, the hydroxyl vibration peaks of HBT and its derivatives have different degrees of variation. The red-shift values of P-TPA, M-TPA, P-DNP and M-DNP are 306.86, 217.36, 79.39 and 49.01 cm^{-1}. For these studied molecules, the order of change for –OH strength is P-TPA>M-TPA>P-DNP>M-DNP. In general, the substitution of electron-withdrawing groups will weaken intramolecular hydrogen bond, and the stronger the electron-withdrawing ability, the more obvious the influence. Substitution with triphenylamine group will obtain better enhancement that substitution of the DNP group.

It is well understood that the absorption and fluorescence properties of compounds are intimately connected to electronic transitions. Consequently, Figure S7 illustrates the highest occupied molecular orbital (HOMO) and the lowest unoccupied molecular orbital (LUMO), allowing for the observation of electron cloud distribution both before and after light excitation. In general, the introduction of the electron donating group can raise the HOMO energy level, which leads to the enhanced electron-giving ability of the compound. And it can also make the energy gap between HOMO and LUMO

decrease, which is favorable to the transition. The substitution of electron- withdrawing groups results in the opposite.

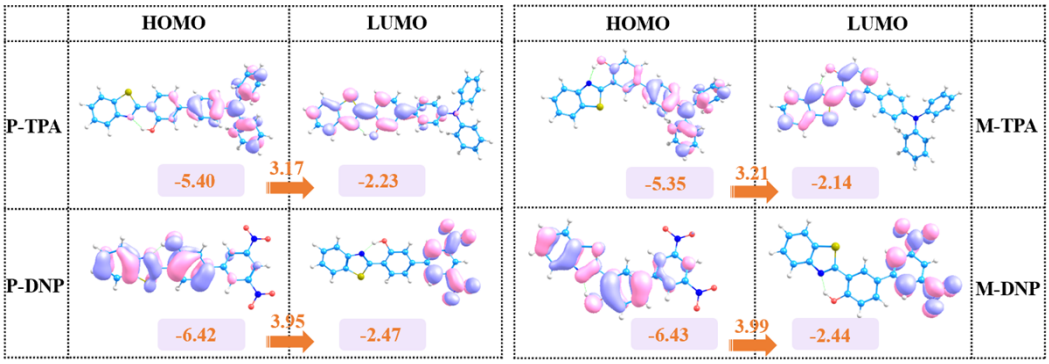

Fig. S7 The frontier molecular orbitals of P-TPA, M-TPA, P-DNP, M-DNP and the corresponding energy and energy gap values (eV)